

Cite this: *Green Chem.*, 2011, **13**, 2116

www.rsc.org/greenchem

PAPER

H₃PW₁₂O₄₀ supported on silica-encapsulated γ -Fe₂O₃ nanoparticles: a novel magnetically-recoverable catalyst for three-component Mannich-type reactions in water

Ezzat Rafiee^{*a,b} and Sara Eavani^a

Received 17th March 2011, Accepted 5th May 2011

DOI: 10.1039/c1gc15291b

A new type of magnetically-recoverable catalyst was synthesized by the immobilization of H₃PW₁₂O₄₀ on the surface of silica-encapsulated γ -Fe₂O₃ nanoparticles. This catalyst was characterized by transmission electron microscopy (TEM), a laser particle size analyzer, infrared spectroscopy (IR) and inductively coupled plasma atomic emission spectroscopy (ICP-AES). The results show that the particles are mostly spherical in shape and have an average size of approximately 94 nm. The characterization data derived from IR spectroscopy reveal that H₃PW₁₂O₄₀ on the support exists in the Keggin structure. The acidity of the catalyst was measured by a potentiometric titration with n-butylamine. To our surprise, this very strong solid acid catalyst showed an excellent distribution of acid sites, suggesting that the catalyst possesses a higher number of surface active sites compared to its homogeneous analogues. The activity of the catalyst was probed through one-pot three-component Mannich-type reactions of aldehydes, amines and ketones in water at room temperature. The excellent conversions show that the catalyst has strong and sufficient acidic sites, which are responsible for its catalytic performance. After the reaction, the catalyst/product separation could be easily achieved with an external magnetic field, and more than 95% of the catalyst could usually be recovered. The catalyst was reused at least five times without any loss of its high catalytic activity.

Introduction

Over the past several past decades, Green Chemistry has demonstrated how fundamental scientific methodologies can protect human health and the environment in an economically beneficial manner. Significant progress is being made in several key research areas, such as catalysis, the design of safer chemicals and environmentally benign solvents.

The application of catalysis to reduced toxicity systems, benign and renewable energy systems, and reaction efficiency makes it a central focus area for green chemistry research in the 21st century. It is possible to prepare heterogeneous analogues of the most commonly used soluble and homogeneous catalysts by their immobilization on various insoluble supports. The use of heterogeneous catalysts in chemical processes would simplify catalyst removal and minimize the amount of waste formed. However, although heterogeneous catalysts can be recovered by filtration or precipitation through adding precipitating agents

to the reaction medium, these methods are time- and energy-consuming. Moreover, a substantial decrease in the activity and selectivity of the immobilized catalyst is frequently observed due to the heterogeneous nature of support materials in reaction media, steric and diffusion factors.¹ A great proportion of active species are deep inside the supporting matrix and thus reactants have limited access to catalytic sites. Therefore, to maintain economic viability, a suitable heterogeneous system must not only minimize the production of waste, but should also exhibit activities and selectivities comparable or superior to existing homogeneous routes.

In an attempt to resolve such problems, nanoparticles (NPs) have been used as alternative soluble matrixes for supporting homogeneous catalysts. When the size of the support materials is decreased to the nanometer scale, the surface area of the NPs increases dramatically. As a consequence, NPs could have a higher catalyst loading capacity and a higher dispersion than many conventional support matrices, leading to an improved catalytic activity of the supported catalysts. However, conventional separation methods may become inefficient for support particle sizes below 100 nm. The incorporation of magnetic NPs (MNPs) such as iron oxide into supports offers a solution to this problem.² The strategy of magnetic separation, taking

^aFaculty of Chemistry, Razi University, Kermanshah, 67149, Iran. E-mail: ezzat_rafiee@yahoo.com, e.rafiei@razi.ac.ir; Fax: +98 831 4274559; Tel: +98 831 4274559

^bKermanshah Oil Refining Company, Kermanshah, Iran

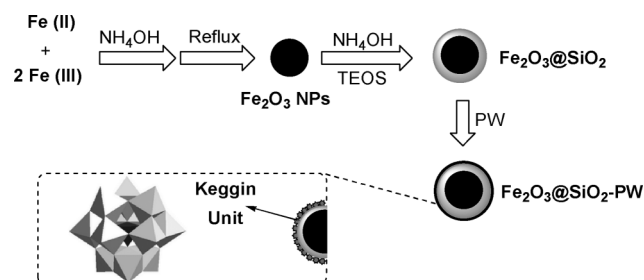
advantage of MNPs, is typically more effective than filtration or centrifugation as it prevents loss of the catalyst. The magnetic separation of MNPs is simple, economical and promising for industrial applications.³ Currently, much attention is focused on the synthesis of magnetic core-shell structures by coating an SiO₂ shell around pre-formed NPs.⁴ Nanosized silica, which is non-toxic and can be grafted with a variety of surface modifiers, has great potential in many applications.⁵

Since Keggin-type heteropoly acids (HPAs) such as H₃PW₁₂O₄₀ (PW) were first commercialized in the industrial research field, a large number of these catalysts have been developed for a wide range of organic reactions in fundamental research.^{6,7} Several advantages to be highlighted of using supported HPAs compared to homogeneous examples include easier recovery and recycling after carrying out reactions, and easier product separation.⁸ However, separation and recovery of the immobilized HPAs are usually performed by filtration or centrifugation, which are not eco-friendly processes.

The immobilization of PW on silica-coated γ -Fe₂O₃ NPs (designed as γ -Fe₂O₃@SiO₂-PW) can be employed to derive a novel heterogeneous catalyst system that possesses both a high separation efficiency and a relatively high surface area to maximize catalyst loading and activity. Certainly, the use of environmentally benign solvents has been another key research area of green chemistry, with great advances being seen in aqueous catalysis. Along this line, we synthesized γ -Fe₂O₃@SiO₂-PW as a novel nanomagnetically-recoverable catalyst and assessed its catalytic activity in Mannich-type reactions in water. Indeed, the venerable Mannich reaction and its variants represent one of the more powerful constructs for alkaloid synthesis.⁹ To the best of our knowledge, this is the first report on the synthesis, characterization and catalytic application of a γ -Fe₂O₃@SiO₂-PW catalyst.

Results and discussion

Scheme 1 presents the synthetic strategy for γ -Fe₂O₃@SiO₂-PW NPs.



Scheme 1 Schematic illustration of the general approach to the synthesis of γ -Fe₂O₃@SiO₂-PW NPs.

Magnetic γ -Fe₂O₃ NPs were prepared through the chemical co-precipitation method. In aerated solutions, an aqueous mixture of ferric and ferrous salts precipitate as an aqueous dispersion of γ -Fe₂O₃ via the addition of strong alkaline solutions in the pH range 7.5–14. In this work, a solution of NH₄OH was used as the alkali source. The chemical reaction of γ -Fe₂O₃ precipitation is given by:



The IR spectrum of the synthesized γ -Fe₂O₃ NPs is shown in Fig. 1. The absorption bands at 449.5, 588.7, 637.8, 799.5 and 900 cm⁻¹ are in good agreement with the IR results reported for pure maghemite (γ -Fe₂O₃).¹⁰

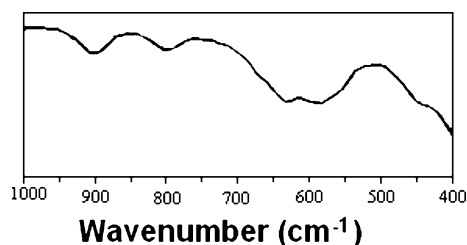


Fig. 1 IR spectrum of γ -Fe₂O₃ NPs.

Sonication of the γ -Fe₂O₃ NP suspension in an alkaline ethanol-water solution of tetraethyl orthosilicate (TEOS) caused the rapid coating of the magnetic cores with silica shells. The outer shell of silica not only improves the dispersibility but also provides suitable sites (Si-OH groups) for surface functionalization with PW. Ultimately, mixing a suspension of γ -Fe₂O₃@SiO₂ with a methanolic solution of PW lead to the formation of γ -Fe₂O₃@SiO₂-PW NPs. Elemental analysis from ICP showed that the W content was 23.7 wt%. Typically, a loading at ca. 31 wt% PW (1.1 mmol g⁻¹) was obtained.

Fig. 2(a) and (b) show the TEM image and size histogram for the γ -Fe₂O₃@SiO₂-PW NPs, respectively. The particle size distribution from the TEM image shows that 66% of NPs are in the range 75–90 nm and that the mean diameter of the observable NPs is 73.5 nm. The size distribution of the γ -Fe₂O₃@SiO₂-PW NPs derived from a laser particle size analyzer, illustrated in Fig. 2(c), indicates that the mean diameter of the particles is 93.8 nm. As shown in the TEM image (Fig. 2(d)), aggregation/coalescence of individual γ -Fe₂O₃ NPs occurred, and that they could have been in an aggregated state during the coating process. Such aggregations form bigger structures with a non-spherical morphology, which causes the difference between the results derived from TEM analysis and the measurements made by the laser particle size analyzer. A typically core-shell structure of a γ -Fe₂O₃@SiO₂-PW NP is shown in Fig. 2(e). The dark core of the γ -Fe₂O₃ and the grey silica shell are clearly observable. The typical silica shell thickness was estimated to be around 10 nm. Due to the strong mass difference between SiO₂ and PW, it could be assumed that the outside darker contrast indicates the shell of PW particles immobilized onto the γ -Fe₂O₃@SiO₂ NPs.

IR spectra of γ -Fe₂O₃@SiO₂, γ -Fe₂O₃@SiO₂-PW and PW samples are shown in Fig. 3. All samples show broad bands at around 1650 cm⁻¹, which are attributed to adsorbed water. The transmission spectrum of γ -Fe₂O₃@SiO₂ shows that the absorption band at 589 cm⁻¹ could be related to the vibration of γ -Fe-O.¹¹ The other peaks at 627 and 895 cm⁻¹ are pure γ -Fe₂O₃.¹⁰ The bands at 1100 cm⁻¹, along with shoulder at 1200 and 461 cm⁻¹, are presumably due to asymmetric stretching and bending modes of Si-O-Si, respectively. The shoulder at 800 cm⁻¹ may be assigned either to a symmetric stretching of Si-O-Si or a stretching vibration of Fe-O bonds. The characteristic band of Si-O-Fe appears at 686 cm⁻¹ in this sample.¹² The PW₁₂O₄₀³⁻ Keggin ion structure is well known and consists of

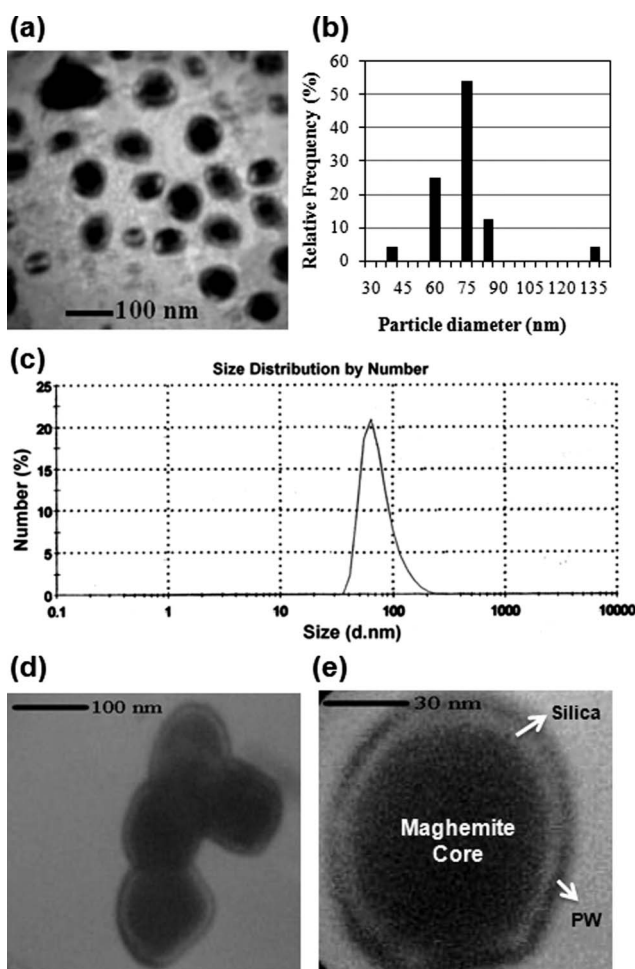


Fig. 2 (a) TEM image, (b) size histogram, (c) grain size distribution, (d) aggregation/coalescence and (e) typical core-shell structure of a $\gamma\text{-Fe}_2\text{O}_3\text{@SiO}_2\text{-PW}$ NP.

a PO_4 tetrahedron surrounded by four W_3O_{13} groups formed by edge-sharing octahedra. These groups are connected to each other by corner-sharing oxygens.¹³ This structure gives rise to four types of oxygen, being responsible for the fingerprint bands of the Keggin ion between 700 and 1200 cm^{-1} . PW shows typical bands for absorptions at 1080 (P–O), 984 (W=O), 896 and 814 (W–O–W) cm^{-1} . In $\gamma\text{-Fe}_2\text{O}_3\text{@SiO}_2\text{-PW}$, the characteristic bands are at the same wavenumbers, with a small shift according to the interaction with the support. The PW band in the 1080 cm^{-1} zone is masked by the Si–O–Si absorption band in the $\gamma\text{-Fe}_2\text{O}_3\text{@SiO}_2\text{-PW}$ spectrum. However, information can still be obtained from the less affected regions, which show an intensity increase of the band at 814 cm^{-1} , and non-overlapped bands at 896 and 984 cm^{-1} that confirm that the PW on the support exists in the Keggin structure.

The zeta potential of the $\gamma\text{-Fe}_2\text{O}_3$ and $\gamma\text{-Fe}_2\text{O}_3\text{@SiO}_2$ samples suspended in aqueous solutions were about -30 and -85 mV, respectively. These results are in good agreement with those reported in the literature¹⁴ and confirm that $\gamma\text{-Fe}_2\text{O}_3$ NPs were successfully covered by an SiO_2 shell. The zeta potential distribution for $\gamma\text{-Fe}_2\text{O}_3\text{@SiO}_2\text{-PW}$ is shown in Fig. 4. 1% of NPs showed a zeta potential of about -29.5 mV, indicating the existence of a few uncovered $\gamma\text{-Fe}_2\text{O}_3$ NPs. Another two

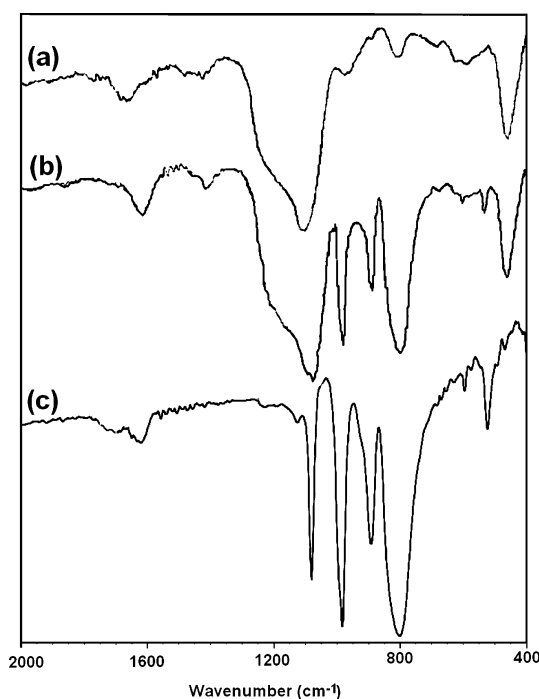


Fig. 3 IR spectra of (a) $\gamma\text{-Fe}_2\text{O}_3\text{@SiO}_2$, (b) $\gamma\text{-Fe}_2\text{O}_3\text{@SiO}_2\text{-PW}$ and (c) PW.

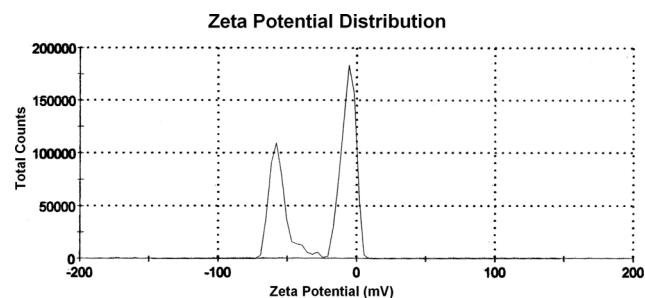
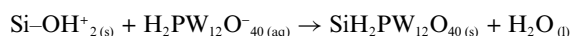
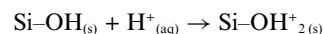
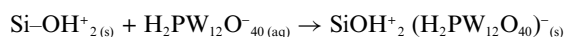


Fig. 4 Zeta potential distribution of $\gamma\text{-Fe}_2\text{O}_3\text{@SiO}_2\text{-PW}$.

peaks at -6.73 (60.3%) and -56.5 (38.6%) mV reveal that two dominate HPA surface complexes exist on the $\gamma\text{-Fe}_2\text{O}_3\text{@SiO}_2$ surface. Clearly the Keggin ion is strongly interacting with the surface hydroxyl groups of the silica.¹⁵ This may occur by an exchange reaction, leading to the formation of water and the replacement of the surface hydroxyl anion by a Keggin anion:



or through interaction of a protonated hydroxyl group (OH_2^+) with the anion:



The present results do not allow a more detailed description of the bonding and structures of the HPA species present on the support surface, and more experiments are needed. However, the shift in zeta potential value compared to $\gamma\text{-Fe}_2\text{O}_3$ and $\gamma\text{-Fe}_2\text{O}_3\text{@SiO}_2$ showed that all of the $\gamma\text{-Fe}_2\text{O}_3\text{@SiO}_2$ NPs are modified with PW.

The nature of the support apparently affects the acidity of the supported HPAs, which was probed by a potentiometric titration with an organic base.⁷ This method, based on the measured potential difference, is mainly determined by the acidic environment around the electrode membrane. The measured electrode potential is an indicator of the acidic properties of the dispersed solid particles. An aliphatic amine, such as *n*-butylamine, with a basic dissociation constant of approximately 10^{-6} , allows the potentiometric titration of strong acids. The titration curves obtained for SiO₂, PW, 40 wt% PW/SiO₂ and γ -Fe₂O₃@SiO₂ are presented in Fig. 5. It is considered that the initial electrode potential (E_i) indicates the maximum strength of the acid sites and that the value from which the plateau is reached (mmol amine per g catalyst) indicates the total number of acid sites that are present in the titrated solid. The acidic strength of the acid sites can be classified according to the following ranges: $E_i > 100$ mV (very strong acid sites), $0 < E_i < 100$ mV (strong acid sites), $-100 < E_i < 0$ mV (weak acid sites) and $E_i < -100$ mV (very weak acid sites).⁷ Bulk SiO₂ presented strong acid sites ($E_i = 78.1$ mV). γ -Fe₂O₃@SiO₂ showed very weak acid sites in comparison with SiO₂. This may be due to the interaction of Si–O–H with γ -Fe₂O₃ and the formation of Si–O–Fe species, as confirmed by IR spectroscopy. The addition of PW to the SiO₂ surface (as described above) should decrease the strength of the acid sites of the PW molecules. This effect depends on the extent of the interaction of PW with the support. According to potentiometric titration curves (Fig. 5), PW presented very strong acidic sites ($E_i = 650$ mV). A 40 wt% PW/SiO₂ sample showed acidic sites with essentially the same maximum strength, which might be an indication of a low interaction level and the formation of predominantly less dispersed intact PW anions on the silica support. Thus, this supported catalyst showed significant leaching of PW in polar solvents. Potentiometric titration results of a γ -Fe₂O₃@SiO₂-PW sample showed that the lower E_i value (450 mV) compared to the PW and 40 wt% PW/SiO₂ samples (compare titration curves of 40 wt% PW/SiO₂ and γ -Fe₂O₃@SiO₂-PW in Fig. 5 and Fig. 6, respectively) may be a consequence of a strong interaction with the support for γ -Fe₂O₃@SiO₂-PW. This interacting species is well dispersed on the support surface and does not leach during the reaction. Additionally, the immobilization of PW on γ -Fe₂O₃@SiO₂ NPs

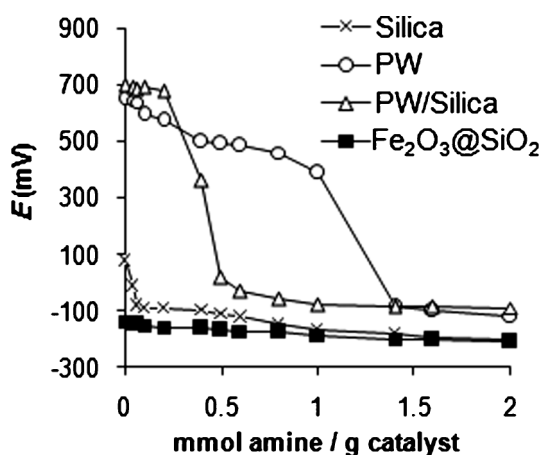


Fig. 5 Potentiometric titration curves of SiO₂, PW, 40 wt% PW/SiO₂ and γ -Fe₂O₃@SiO₂.

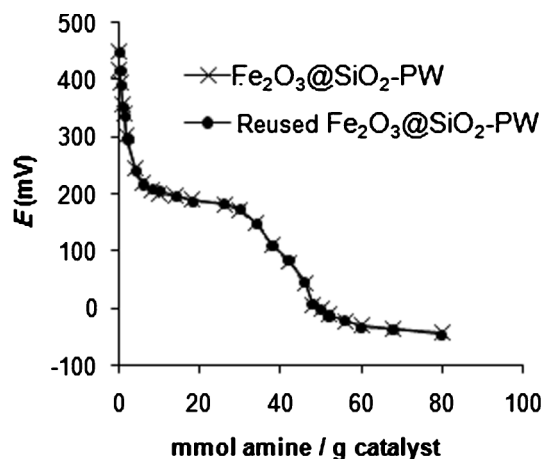


Fig. 6 Potentiometric titration curves of γ -Fe₂O₃@SiO₂-PW and reused γ -Fe₂O₃@SiO₂-PW.

considerably enhanced the dispersion of acidic protons to 48 mmol g⁻¹ catalyst (Fig. 6). Therefore, a larger fraction of active sites are exposed to the surface, and this catalyst may exhibit excellent activity in organic reactions, even with a low catalyst loading.

The activity of the novel catalyst was probed through a one-pot three-component Mannich-type reaction of benzaldehyde, aniline and cyclohexanone as model substrates. Without the addition of catalyst, only the imine was formed through the condensation of benzaldehyde and aniline.¹⁶ γ -Fe₂O₃@SiO₂ NPs and PW produced the Mannich product with 65 and 85% yields, but the imine also obtained in 20 and 15% yield, respectively (Table 1, entries 1 and 2). Yet, their combination in the form of γ -Fe₂O₃@SiO₂-PW increased the yield of the Mannich product to 98% in a significantly shorter reaction time (Table 1, entry 3). Besides, this novel catalyst showed a higher yield and selectivity in comparison with 40 wt% PW/SiO₂ (Table 1, entry 4). This result indicated that the catalytic activity should be directly proportional to the number of surface acid sites, which are the ones accessible to the reactants. To investigate the effect of catalyst loading, the model reaction was carried out in the presence of different amounts of catalyst. The best result was obtained in the presence of just 0.005 g of γ -Fe₂O₃@SiO₂-PW, and the use of higher amounts of catalyst slightly decreased the reaction time (Table 1, entries 5–9).

Recycling experiments were performed by the Mannich condensation of benzaldehyde, aniline and cyclohexanone in water. The model reaction was carried out by using 0.1 g of catalyst and the experiments were suitably scaled up (Fig. 7(a)). When the reaction was complete, γ -Fe₂O₃@SiO₂-PW could be placed on the side wall of the reaction vessel with the aid of an external magnet (Fig. 7(b)) and water was removed from the mixture to leave a residue (including the product and catalyst) (Fig. 7(c)). Then, the product was dissolved in ethanol and the catalyst easily separated from the product by attaching an external magnet onto the reaction vessel, followed by decantation of the product solution (Fig. 7(d)). The remaining catalyst was washed with diethyl ether to remove the residual product, dried under vacuum and reused in a subsequent reaction. More than 95% of the catalyst could usually be recovered from each reaction. In a test of five cycles, the catalyst could be

Table 1 Catalytic activity of $\gamma\text{-Fe}_2\text{O}_3\text{@SiO}_2\text{-PW}$ in the model reaction

Entry	Catalyst	Time (min)/Yield (%) ^a	
		Imine	Mannich product
1	$\gamma\text{-Fe}_2\text{O}_3\text{@SiO}_2$ (0.04 g)	180/20	180/65
2	PW (0.04 g)	60/15	60/85
3	$\gamma\text{-Fe}_2\text{O}_3\text{@SiO}_2\text{-PW}$ (0.04 g)	5/0	5/98
4	40 wt% PW/SiO ₂ (0.04 g) ^b	80/30	80/65
5	$\gamma\text{-Fe}_2\text{O}_3\text{@SiO}_2\text{-PW}$ (0.08 g)	5/0	5/98
6	$\gamma\text{-Fe}_2\text{O}_3\text{@SiO}_2\text{-PW}$ (0.02 g)	8/0	8/98
7	$\gamma\text{-Fe}_2\text{O}_3\text{@SiO}_2\text{-PW}$ (0.01 g)	12/0	12/98
8	$\gamma\text{-Fe}_2\text{O}_3\text{@SiO}_2\text{-PW}$ (0.005 g)	15/0	15/98
9	$\gamma\text{-Fe}_2\text{O}_3\text{@SiO}_2\text{-PW}$ (0.003 g)	30/15	30/85

^a Isolated yield. ^b W content in anhydrous catalyst from ICP is 29.6 wt%.⁷

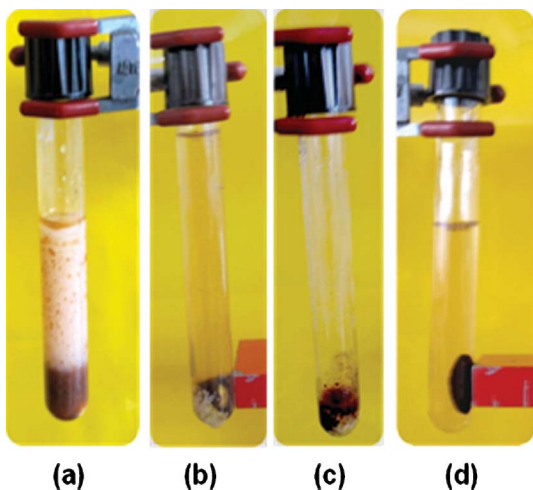


Fig. 7 Separation of the $\gamma\text{-Fe}_2\text{O}_3\text{@SiO}_2\text{-PW}$ catalyst from the reaction mixture using an external magnet.

reused without any significant loss to its catalytic activity (Fig. 8). The potentiometric titration curve of the reused catalyst showed that all of its acidic sites were preserved during five cycles (Fig. 6). According to ICP-AES results, PW leaching was negligible.

The reaction was extended to a series of aldehydes, ketones and amines to explore the generality of this catalytic system (Table 2). In the cases of β -aminocyclohexanones, the stereoselectivity was determined by ¹H NMR spectroscopy and by comparison with known compounds (Table 2, entries 1–3).¹⁶ Selectivity for the *anti*-isomer was favored in all cases. Aliphatic aldehyde and amine substrates afforded the corresponding products in good yields (Table 2, entries 9 and 10). Previous approaches gave negative results or very poor yields for similar reactions.¹⁷

It is worth mentioning that the *ortho*-substituted aromatic amines, which generally appeared in only trace amounts or even not at all because of the large steric hindrance,¹⁸ also afforded

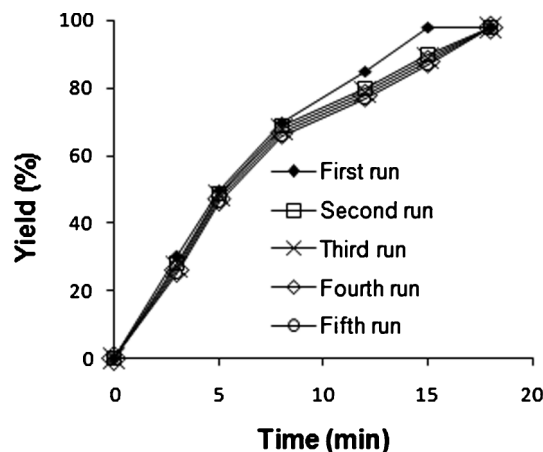


Fig. 8 The reusability of $\gamma\text{-Fe}_2\text{O}_3\text{@SiO}_2\text{-PW}$.

the corresponding Mannich products in good to excellent yields (Table 2, entries 11 and 12).

Experimental

General

The reagents and solvents used in this work were obtained from Fluka, Aldrich or Merck and were used without further purification. TEM analyses were performed using a TEM microscope (Philips CM 120 KV, The Netherlands). The size distribution and zeta potential of the samples were obtained using a laser particle size analyzer (HPPS5001, Malvern, UK). IR spectra were recorded as KBr pellets using a Shimadzu 470 spectrophotometer. The tungsten (W) content in the catalyst was measured by ICP-AES on a Spectro Ciros CCD spectrometer. The potential variation was measured with a Hanna 302 pH meter and a double junction electrode.

Table 2 The synthesis of various β -amino ketones *via* Mannich reactions

$$R^1CHO + R^2NH_2 + R^3\text{---}CH_2\text{---}C(=O)R^4 \xrightarrow[H_2O (5 \text{ mL}), \text{ r.t.}]{Fe_2O_3@SiO_2\text{-PW} (0.005 \text{ g})} R^1\text{---}CH(R^3)\text{---}CH(R^2)N\text{---}R^4$$

Entry	R ¹	R ²	R ³	R ⁴	Time/min	Yield (%) ^a
1	Ph	Ph	-(CH ₂) ₄ -		15	98 ^b
2	Ph	4-ClC ₆ H ₄	-(CH ₂) ₄ -		45	96 ^b
3	4-CH ₃ OC ₆ H ₄	4-ClC ₆ H ₄	-(CH ₂) ₄ -		50	91 ^b
4	4-CH ₃ OC ₆ H ₄	Ph	H	Ph	25	90
5	4-ClC ₆ H ₄	4-ClC ₆ H ₄	H	Ph	20	92
6	4-CH ₃ C ₆ H ₄	Ph	H	Ph	25	90
7	Ph	Ph	H	4-CH ₃ C ₆ H ₄	40	80
8	Ph	Ph	H	4-ClC ₆ H ₄	30	90
9	n-C ₃ H ₇	Ph	H	Ph	120	83
10	Ph	n-C ₄ H ₉	H	Ph	50	85
11	Ph	2-CH ₃ C ₆ H ₄	H	Ph	180	71
12	Ph	2-FC ₆ H ₄	H	Ph	65	95

^a Isolated yield. ^b *Anti/syn* ratio: 67/33, 63/37 and 68/32 for entries 1–3, respectively.

Preparation of the catalyst

The γ -Fe₂O₃ NPs were synthesized by a chemical co-precipitation technique of ferric and ferrous ions in an alkaline solution. FeCl₂·4H₂O (2.0 g) and FeCl₃·6H₂O (5.4 g) were dissolved in water (20 mL) separately, followed by the two iron salt solutions being mixed under vigorous stirring. An NH₄OH solution (0.6 M, 200 mL) was then added to the stirring mixture at room temperature, immediately followed by the addition of a concentrated NH₄OH solution (25% w/w, 30 mL) to maintain the reaction pH between 11 and 12. The resulting black dispersion was continuously stirred for 1 h at room temperature and then heated to reflux for 1 h to yield a brown dispersion. The MNPs were then purified by a four times repeated centrifugation (4000–6000 rpm, 30 min), decantation and redispersion cycle until a stable brown magnetic dispersion (pH 9.2) was obtained (mean diameter = 65.5 nm). Coating of a layer of silica on the surface of the γ -Fe₂O₃ NPs was achieved by pre-mixing (ultrasonic) a dispersion of the purified NPs (8.5% w/w, 20 mL) obtained previously with ethanol (80 mL) for 1 h at 40 °C. A concentrated ammonia solution was added and the resulting mixture stirred at 40 °C for 30 min. Subsequently, TEOS (1.0 mL) was charged to the reaction vessel and the mixture continuously stirred at 40 °C for 24 h. The silica-coated NPs were collected using a permanent magnet, followed by washing three times with ethanol, diethyl ether and drying in a vacuum for 24 h (mean diameter = 79.3 nm).

0.7 g of PW was dissolved in 5 mL of dry methanol. This solution was added dropwise to a suspension of 1.0 g γ -Fe₂O₃@SiO₂ in methanol (50 mL) while being dispersed by sonication. The mixture was heated at 70 °C for 72 h under vacuum while being mechanically stirred to obtain γ -Fe₂O₃@SiO₂-PW NPs. The catalyst was collected by a permanent magnet and dried in a vacuum overnight.

Typical procedure for Mannich reactions

Typically, to a mixture of aldehyde (1 mmol), amine (1 mmol), ketone (2 mmol) and H₂O (5 mL) was added the catalyst

(0.005 g). The reaction mixture was vigorously stirred for the period of time listed in Table 2. The progress of the reaction was monitored by TLC. When the reaction was complete, γ -Fe₂O₃@SiO₂-PW could be placed on the side wall of the reaction vessel with the aid of an external magnet, and water was removed from the mixture to leave a residue (including the product and catalyst). Then, the product was dissolved in ethanol and the catalyst easily separated from the product by attaching an external magnet onto the reaction vessel, followed by decantation of the product solution. This solution was concentrated at room temperature to generate the crude product. The crude products were purified either by crystallization from ethanol or by column chromatography on silica gel using ethyl acetate/hexane as the eluent. All products were identified by comparing of their spectral data with those of authentic samples.^{16,19}

Conclusions

The combination of the magnetic separation of γ -Fe₂O₃@SiO₂ NPs and the special properties of PW provide a good opportunity to design and synthesize γ -Fe₂O₃@SiO₂-PW as an efficient nanocatalyst possessing strong and sufficient acidic sites to be responsible for excellent conversion values of products. More importantly, γ -Fe₂O₃@SiO₂-PW is intrinsically heterogeneous and recovered simply using an external magnetic field. The isolated catalyst was reused at least five times without any loss of its catalytic activity, suggesting that even a small amount of the catalyst has stable acidic sites for several cycles of an organic synthesis. As a consequence, MNPs could be an ideal support for the immobilization of other HPA catalysts. In addition to Mannich reactions, such environmentally benign catalysts should find application in a wide range of other important acid-catalyzed organic reactions.

This study is an initial attempt towards the synthesis of nanomagnetically-recoverable HPA-based catalysts. Modification of the synthetic approach, and the preparation, properties and applications of other γ -Fe₂O₃@SiO₂-HPA NPs are in progress, and will be reported in due course.

Acknowledgements

The authors thank the Razi University Research Council and Kermanshah Oil Refining Company for their support of this work.

References

- 1 N. E. Leadbeater and M. Marco, *Chem. Rev.*, 2002, **102**, 3217; B. M. L. Dioso, I. F. J. Vankelecom and P. A. Jacobs, *Adv. Synth. Catal.*, 2006, **348**, 1413.
- 2 D. Astruc, F. Lu and J. R. Aranzaes, *Angew. Chem., Int. Ed.*, 2005, **44**, 7852.
- 3 Y. Zhang and C. Xia, *Appl. Catal., A*, 2009, **366**, 141; L. Mámami, A. Heydari and M. Sheykhan, *Appl. Catal., A*, 2010, **384**, 122; F. Šulek, Ž. Knez and M. Habulin, *Appl. Surf. Sci.*, 2010, **256**, 4596.
- 4 M. Benaglia, A. Puglisi and F. Cozzi, *Chem. Rev.*, 2003, **103**, 3401; F. Cozzi, *Adv. Synth. Catal.*, 2006, **348**, 1367.
- 5 Y. Piao, A. Burns, J. Kim, U. Wiesner and T. Hyeon, *Adv. Funct. Mater.*, 2008, **18**, 3745.
- 6 T. Okuhara, N. Mizuno and M. Misono, *Appl. Catal., A*, 2001, **222**, 63; E. Rafiee, S. Eavani, S. Rashidzadeh and M. Joshaghani, *Inorg. Chim. Acta*, 2009, **362**, 3555.
- 7 E. Rafiee, M. Joshaghani, S. Eavani and S. Rashidzadeh, *Green Chem.*, 2008, **10**, 982.
- 8 P. M. Rao, A. Wolfson, S. Kababya, S. Vega and M. V. Landau, *J. Catal.*, 2005, **232**, 210; H. Firouzabadi and A. A. Jafari, *J. Iranian Chem. Soc.*, 2005, **2**, 85.
- 9 A. L. Simplicio, J. M. Clancy and J. F. Gilmer, *Int. J. Pharm.*, 2007, **336**, 208.
- 10 E. Darezereshki, M. Ranjbar and F. Bakhtiari, *J. Alloys Compd.*, 2010, **502**, 257.
- 11 C. He, T. Sasaki, Y. Shimizu and N. Koshizaki, *Appl. Surf. Sci.*, 2008, **254**, 2196.
- 12 K. C. Barick, B. S. D. Ch. S. Varaprasad and D. Bahadur, *J. Non-Cryst. Solids*, 2010, **356**, 153.
- 13 M. T. Pope, in *Heteropoly and Isopoly Oxometalates*, Springer-Verlag, Berlin, 1983, p. 23.
- 14 S. L. C. Pinho, G. A. Pereira, P. Voisin, J. Kassem, V. Bouchaud, L. Etienne, J. A. Peters, L. Carlos, S. Mornet, C. F. G. C. Geraldés, J. Rocha and M. H. Delville, *ACS Nano*, 2010, **4**, 5339.
- 15 R. L. McCormick, S. K. Boonrueng and A. M. Herring, *Catal. Today*, 1998, **42**, 145.
- 16 E. Rafiee, S. Eavani, F. Khajooei Nejad and M. Joshaghani, *Tetrahedron*, 2010, **66**, 6858.
- 17 W. B. Yi and C. Cai, *J. Fluorine Chem.*, 2006, **127**, 1515; W. Shen, L. M. Wang and H. Tian, *J. Fluorine Chem.*, 2008, **129**, 267.
- 18 Z. Li, X. Ma, J. Liu, X. Feng, G. Tian and A. Zhu, *J. Mol. Catal. A: Chem.*, 2007, **272**, 132; M. Kidwai, N. K. Mishra, V. Bansal, A. Kumar and S. Mozumdar, *Tetrahedron Lett.*, 2009, **50**, 1355; G. P. Lu and C. Cai, *Catal. Commun.*, 2010, **11**, 745.
- 19 H. Zeng, H. Li and H. Shao, *Ultrason. Sonochem.*, 2009, **16**, 758.